Supporting Information

Construction of a flow-through catalytic reactor employing O_3-Fe/TiO_2 for efficient catalytic ozonation disinfection

Jiaxuan Li,[a] Xin Chen,[a] Siyu Li,[a] Kunrong Mei,[bc] Lequan Liu*[a] and Jinhua Ye[ad]

[a] Advanced Catalytic Materials Research Center, School of Material Science and Engineering, Tianjin University, Tianjin 300072, P. R. China

[b] Tianjin Key Laboratory for Modern Drug Delivery and High Efficiency, School of Pharmaceutical Science and Technology, Tianjin University, Tianjin 300072, P. R. China

[c] Key Laboratory of Systems Bioengineering, Ministry of Education, Tianjin University, Tianjin 300072, P. R. China

[d] International Center for Materials Nanoarchitectonics (WPI-MANA), National Institute for Materials Science (NIMS), 1-1 Namiki, Tsukuba 305-0044, Japan

*Corresponding Author. E-mail address: Lequan.Liu@tju.edu.cn

Content in this SI files

Text S1. Materials and Reagents.

$TiCl_4$ (Shanghai Macklin Biochemical Technology Co., Ltd 99.5%), ethylene glycol (Tianjin Heowns Biochem Technologies. Llc., 98.0%), $FeCl_3 \bullet 6H_2O$ (Sinopharm Group Co., Ltd, 99.0%), 5,5-dimethyl-1-pyrroline (Dojindo LABORATORIES Co., Inc., 97%, DMPO). *p*-benzoquinone (97%, *P*-BQ), dimethyl sulfoxide (99.95%, DMSO), D-mannitol (98%) and 2,2,6,6-tetramethyl-4-piperidinol (98%, TEMP) are purchased from Aladdin Co. Ltd., China. All chemicals are used without further purification.

Text S2. Material Characterizations.

The crystallographic structure of the catalysts was characterized by X-ray diffraction (XRD) analysis using Cu-K_α radiation (D8Advanced, Bruker, Germany) with a scanning rate of 10° min^{-1}. The morphology of the samples was obtained by field emission scanning electron microscopy (SEM, Apreo S LoVac, FEI, America) and by transmission electron microscopy (TEM) with an acceleration voltage of 200 kV (Tecnai G2 F20, FEI, America), followed by energy dispersion spectrometry (EDS) to detect the elements content in the samples. The light absorption spectra were recorded by UV-Vis diffuse reflectance spectrophotometer (UV-Vis DRS) at wavelength range of 200-800 nm (UV-2600, Shimadzu, Japan). $BaSO_4$ was used as reflectance reference for the UV-Vis spectrophotometer. The specific Brunauer-Emmett-Teller (BET) analysis was conducted using a Quantachrome Autosorb-iQ instrument (Thermo Scientific, USA). X-ray photoelectron spectroscopy (XPS) was analyzed by a Thermo ESCALAB 250xi spectrometer at a spot size of 500 μm, using an Al K_α source with a resolution of 0.05 eV. The electron paramagnetic resonance (EPR) measurements were performed on an EPR spectrometer (JES-FA 200, JEOL, Japan) with a modulation frequency of 100 kHz and a microwave power of 1.0 mW. FTIR spectra were

recorded on a Nicolet-6700 spectrometer. Raman measurements were carried out on HORIBA Xplora PLUS.

Text S3. Electrochemical measurements.

Cyclic voltammetry (CV) measurements were performed on the CHI 760E electrochemical workstation (Shanghai Chenhua Apparatus Corporation). A standard three-electrode system was used, consisting of a glassy carbon electrode (3 mm diameter) as the working electrode, a saturated Ag/AgCl electrode as the reference electrode, and platinum wire as the counter electrode. To make the working electrodes, 50 mg of catalysts and 20 μL of Nafion solution (5 wt%) were dispersed in 0.5 mL of ethanol which was ultrasonicated to yield a homogeneous ink. 5 μL of the above catalyst ink droplets to the glassy carbon electrode. CV tests were conducted in 1 M Na_2SO_4. Before measurement, the electrolyte solution is saturated with high-purity nitrogen. The CV curves were operated between -0.6 V and 1.5 V with a sweep rate of 50 mV s^{-1}.

Text S4. Raman spectroscopy measurements.

Raman spectroscopy was conducted on DXR Smart Raman (Thermo fisher) in the absence and presence of ozone. In a typical procedure, 0.1 g of catalyst was added to 3 mL water and gaseous ozone was fed into it for 15 minutes. The suspension was immediately placed into the reaction cell, and scanned from 400 to 1200 cm^{-1}.

Text S5. Electron paramagnetic resonance (EPR) measurements.

The electron paramagnetic resonance (EPR) using the JES-FA 200 spectrometer (JEOL, Japan) was utilized to detect free radical species. For this, 30 mg of the catalyst was dissolved in 3 ml of

deionized water. After ultrasonic dispersion for 30 minutes, ozone at the experimental concentration was introduced. Following the trapping agents DMPO or TEMP were promptly added and mixing well, the sample was placed in the EPR cavity for testing.

Text S6. Quantitative analysis of formed ROS.

Using coumarin (COU) as a probe, we quantity the yields of •OH which facilitated the generation of fluorescent 7-hydroxycoumarin (7-HC). Specifically, following an ozone pre-purge, 10 mL of coumarin solution (300 mg/L) was introduced into a 90 mL reaction mixture. The mixture was swiftly quenched with 10.0 mM Na_2SO_3 solution and then filtered through a 0.22-μm PTFE membrane to eliminate any potential interference during subsequent analysis. Utilizing a Fluorolog-3 fluorescence spectrometer (HORIBA Scientific, USA), we precisely quantified the concentration of 7-HC by measuring its fluorescence intensity at 456 nm.

Additionally, to assess the yield of $O_2^{\bullet-}$, we employed 4-chloro-7-nitrobenzo-2-oxa-1,3-diazole (NBD-Cl) as a probe, which reacts with $O_2^{\bullet-}$ to produce a fluorescent superoxide-substituted product. The fluorescence intensity of this product was recorded using the same Fluorolog-3 fluorescence spectrometer (HORIBA Scientific, USA), by capturing its emission spectrum upon excitation at 550 nm.

To quantitatively measure the yield of $^1O_2$, we adopted the 1,3-diphenylisobenzofuran (DPBF) conversion method. Initially, DPBF and Fe/TiO_2 solutions were prepared at a concentration of 0.5 mg/mL each. Following an ozone pre-purge, 5 mL of Fe/TiO_2 was combined with 1 mL of DPBF solution. Subsequently, 1 mL aliquots of this mixture were withdrawn and diluted with 4 mL of

acetonitrile for absorbance measurements, allowing for the accurate determination of $^1O_2$ generation.

Text S7. Quenching tests.

A total of 0.50 g of Fe/TiO_2 was respectively added into 20 mL of trapping agents solution (10 mM of *p*-benzoquinone (*P*-BQ), 2,2,6,6-tetramethylpiperidine (TEMP), D-mannitol, and dimethyl sulfoxide (DMSO)) and ultrasonicated for 30 min. The suspension was then loaded on polyurethane foam, followed by drying in air at 60 °C for 30 min. The next steps were the same as catalytic ozonation disinfection.

Text S8. Other analytical methods.

The density of the surface hydroxyl group is measured according to the saturation deprotonation method, a process in which the surface acid-base reaction reaches saturation. In this method, 0.3 g of catalysts were added to a series of NaOH solutions (50 mL each, with concentrations ranging from 2 to 100 mM). After being shaken at 25 °C for more than 4 h, the solution was filtered with 0.45 μm acetate membrane. The supernatant was titrated with a standard HNO_3 solution to determine the residual NaOH. As the acidic hydroxyl groups react with NaOH, their density can be readily quantified by the NaOH consumption. Based on the principle of charge balance, the acidic and basic hydroxyl groups should be quantitatively equal. Thus, the total density of the surface hydroxyl groups is two times that of the acidic ones.

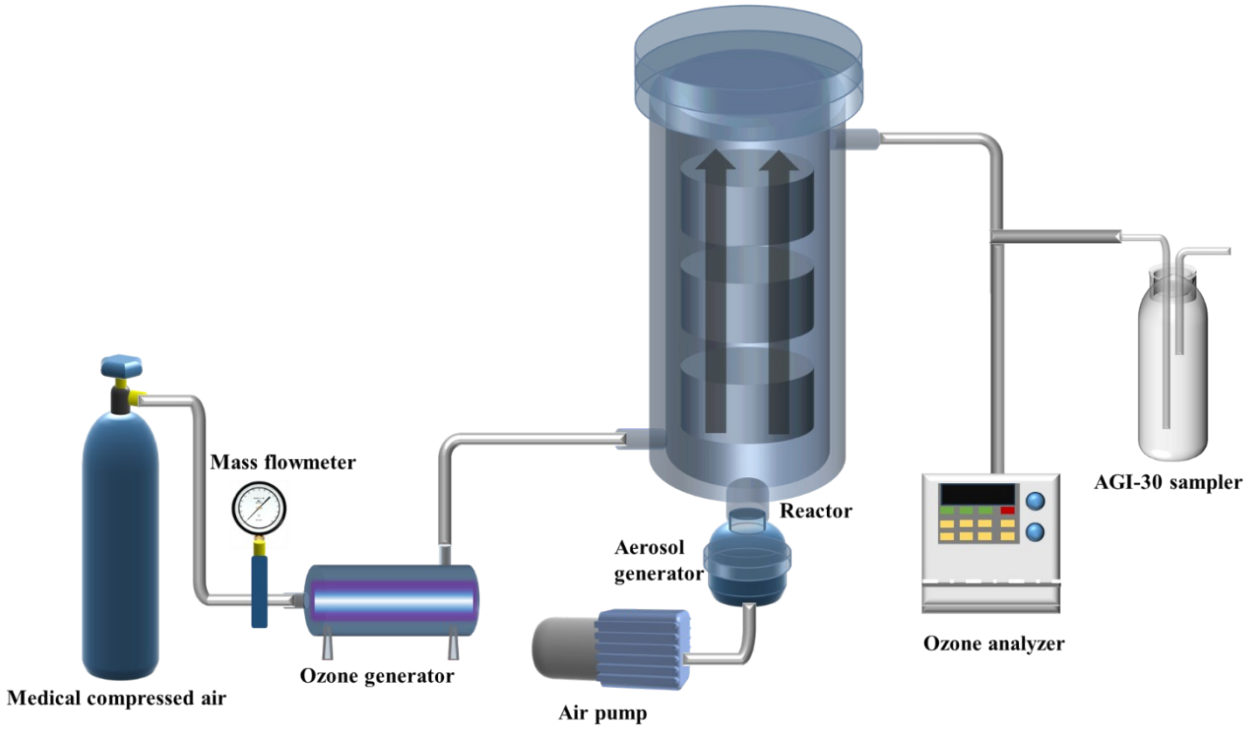

Fig. S1. The schematic experimental setup.

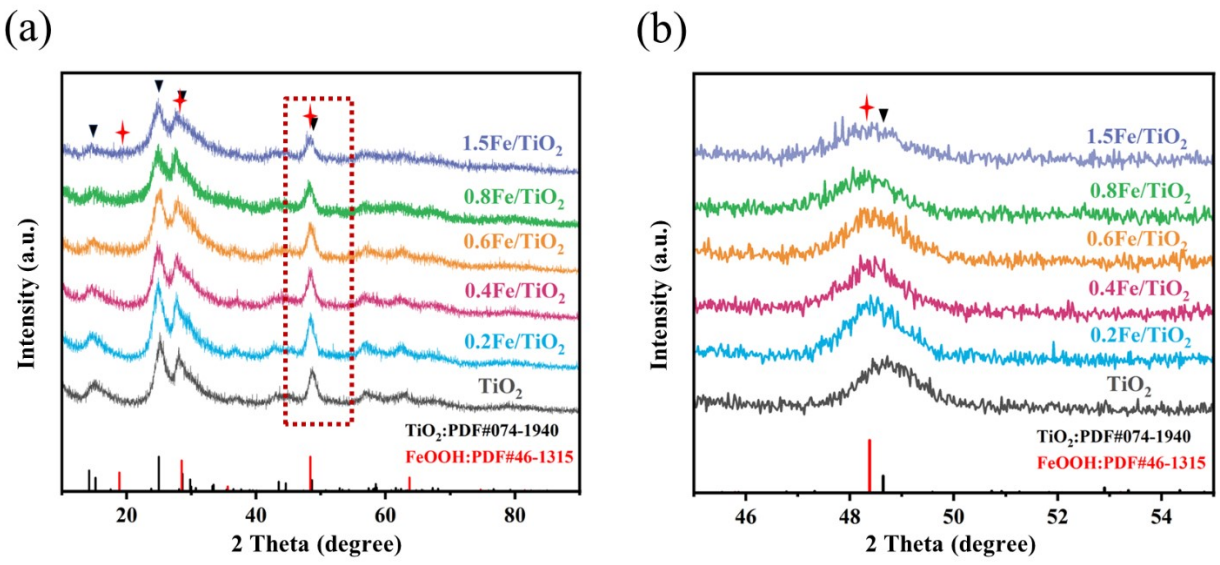

Fig. S2. (a) XRD patterns of pure TiO_2 and (x)Fe/TiO_2. (b) is the slow scan XRD pattern of the dotted line frame in (a).

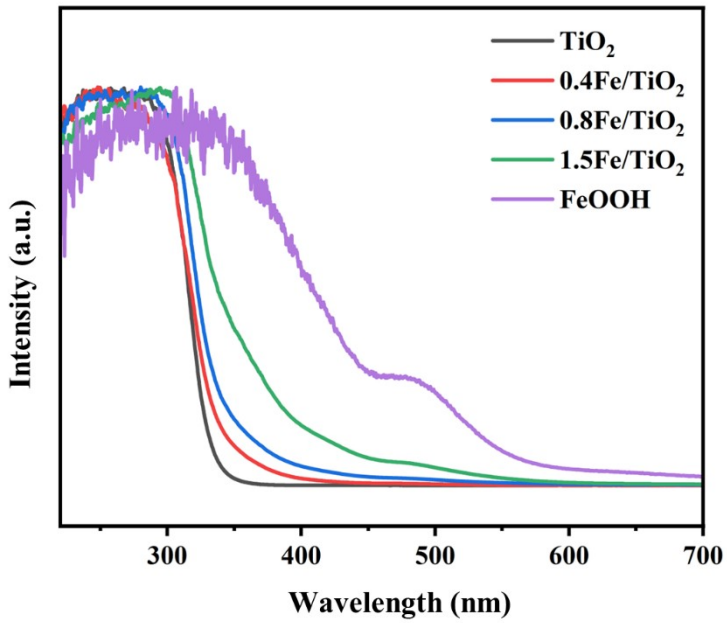

Fig. S3. UV-vis spectra of TiO_2, (x)Fe/TiO_2 and FeOOH.

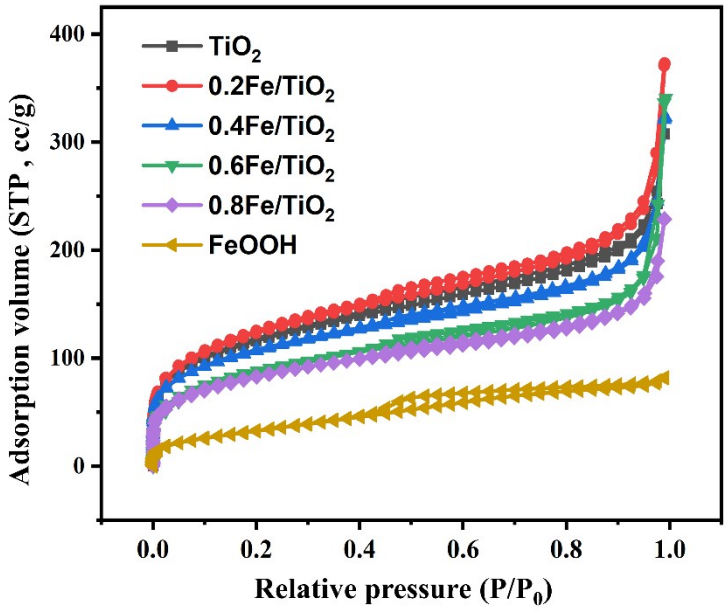

Fig. S4. Nitrogen adsorption–desorption isotherm of TiO_2, (x)Fe/TiO_2 and FeOOH.

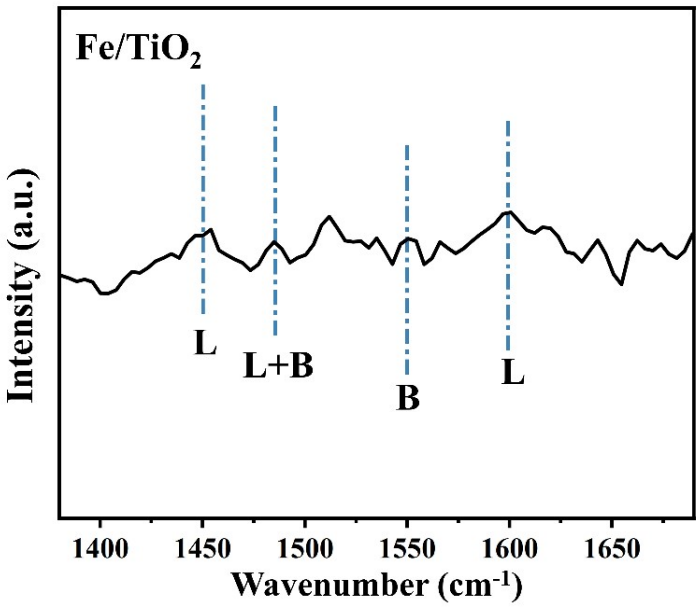

Fig. S5. Pyridine-FTIR of Fe/TiO_2.

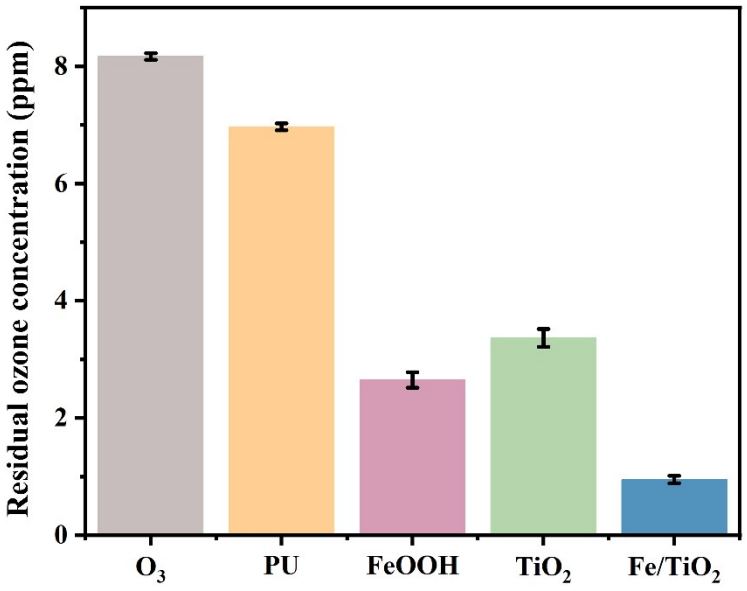

Fig. S6. Residual O_3 concentration under TiO_2, Fe/TiO_2 and FeOOH during the catalytic ozonation disinfection.

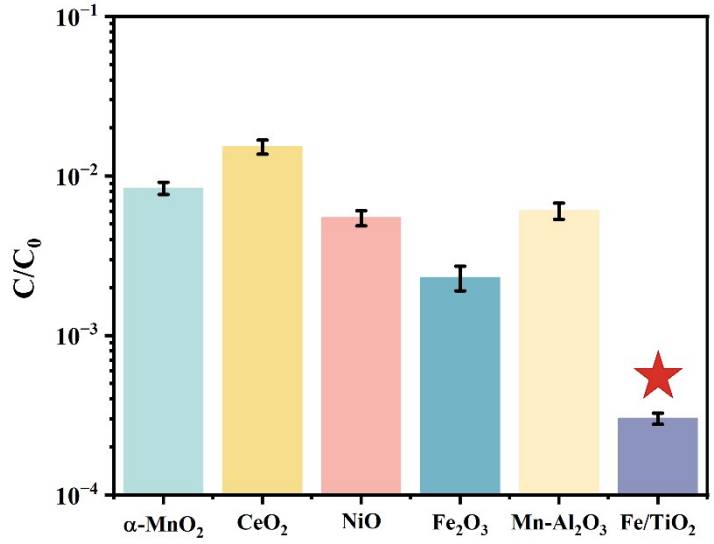

Fig. S7. The bioaerosols disinfection efficiency of Fe/TiO_2 and other prevailing metal-based catalysts.

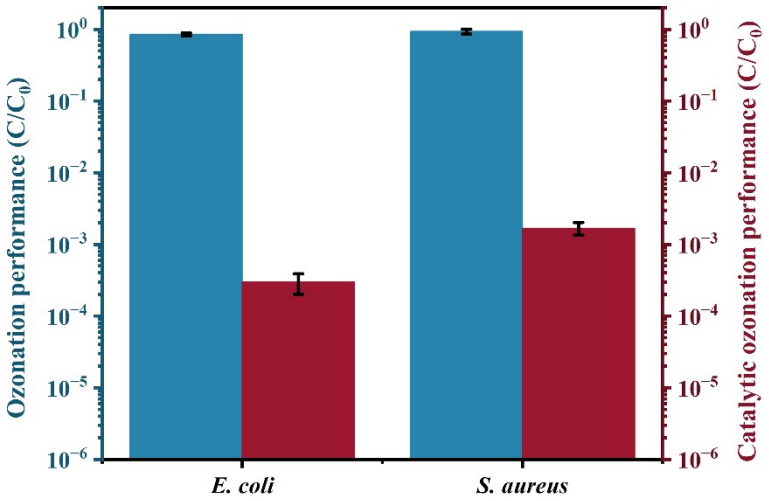

Fig. S8. Effect of bacteria species on inactivation performance. The blue bar represents the ozonation performance, and the red bar represents the catalytic ozonation performance.

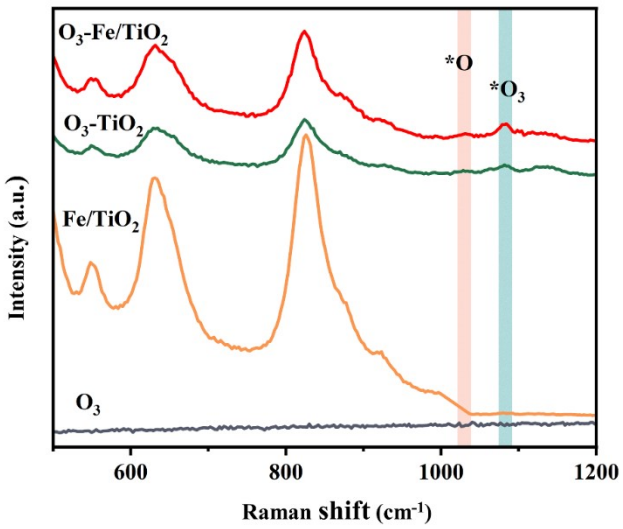

Fig. S9. In-situ Raman spectra of O_3, Fe/TiO_2, O_3-TiO_2, and O_3-Fe/TiO_2.

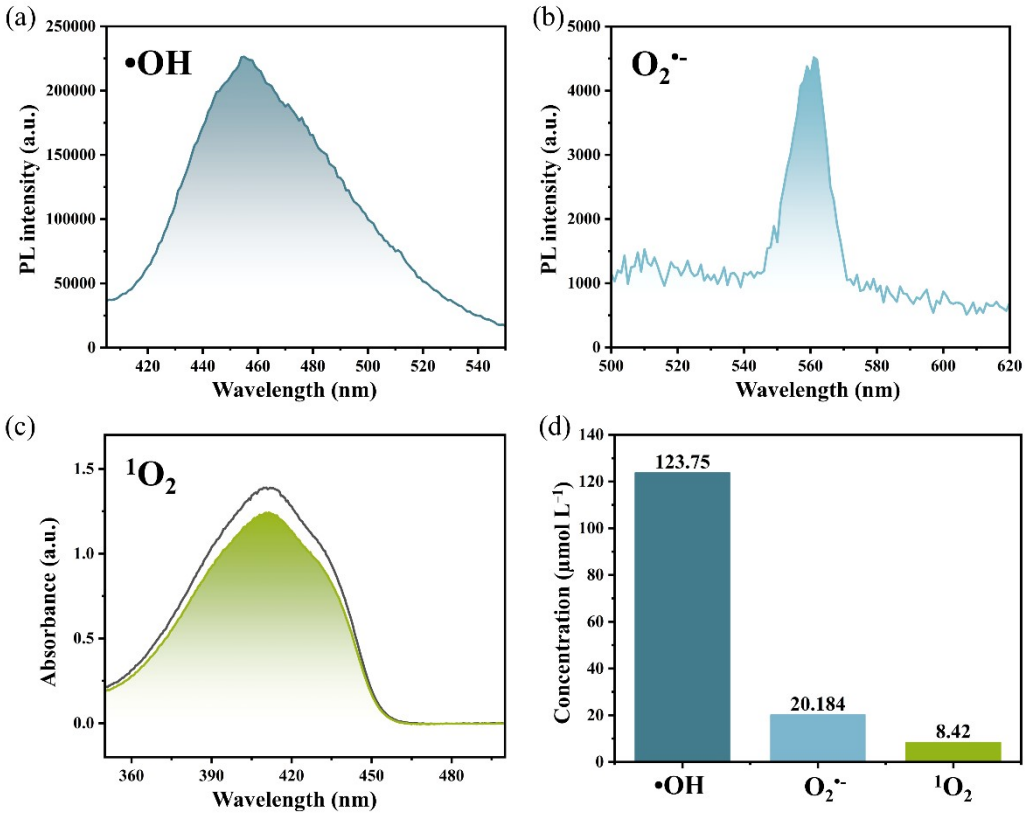

Fig. S10. Fluorescence spectra of coumarin (a) and NBD-Cl (b) after exposing O_3-Fe/TiO_2 system. (c) UV–visible spectra of DPBF solution before and after exposing

O_3-Fe/TiO_2 system. (d) Quantitative determination of different ROS species.

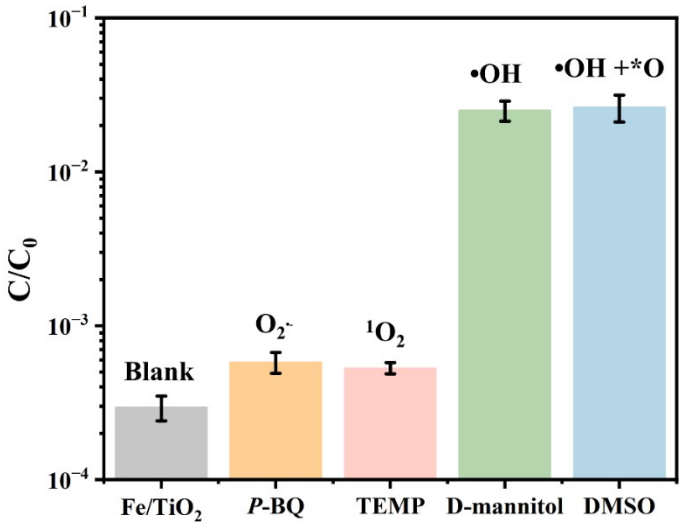

Fig. S11. Quenching tests of active species during the O_3-Fe/TiO_2 catalytic ozonation disinfection.

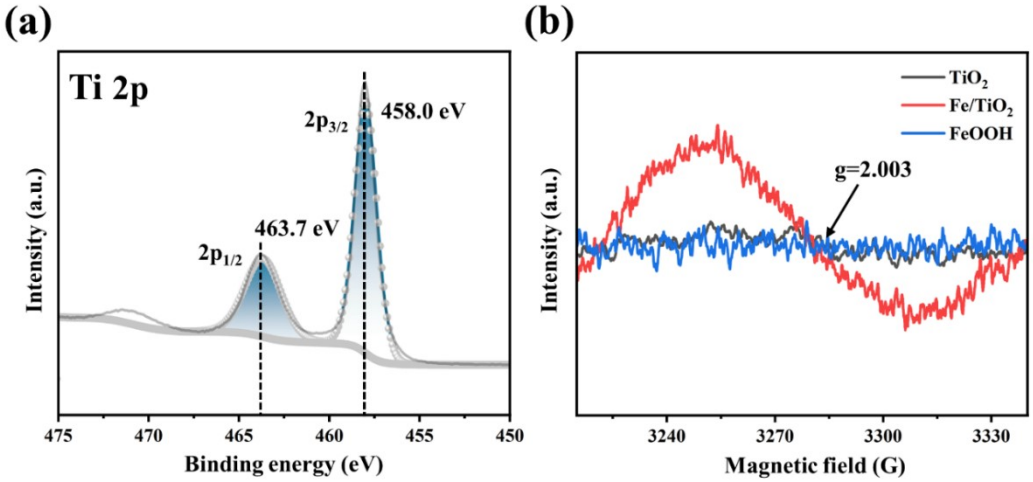

Fig. S12. (a) XPS spectra of Ti 2p for Fe/TiO_2. (b) EPR spectra of TiO_2, Fe/TiO_2 and FeOOH.

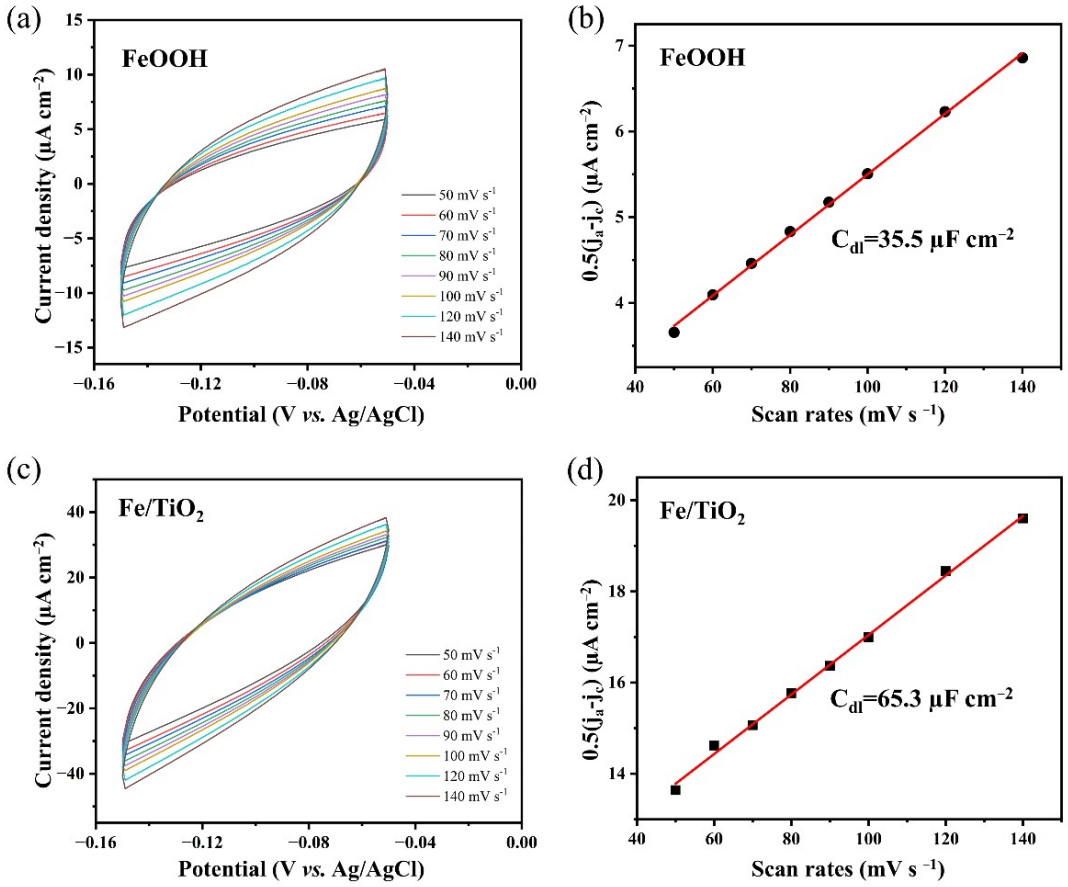

Fig. S13. CV curves and the derived C_{dl} value of (a), (b) FeOOH, and (c), (d) Fe/TiO_2 respectively.

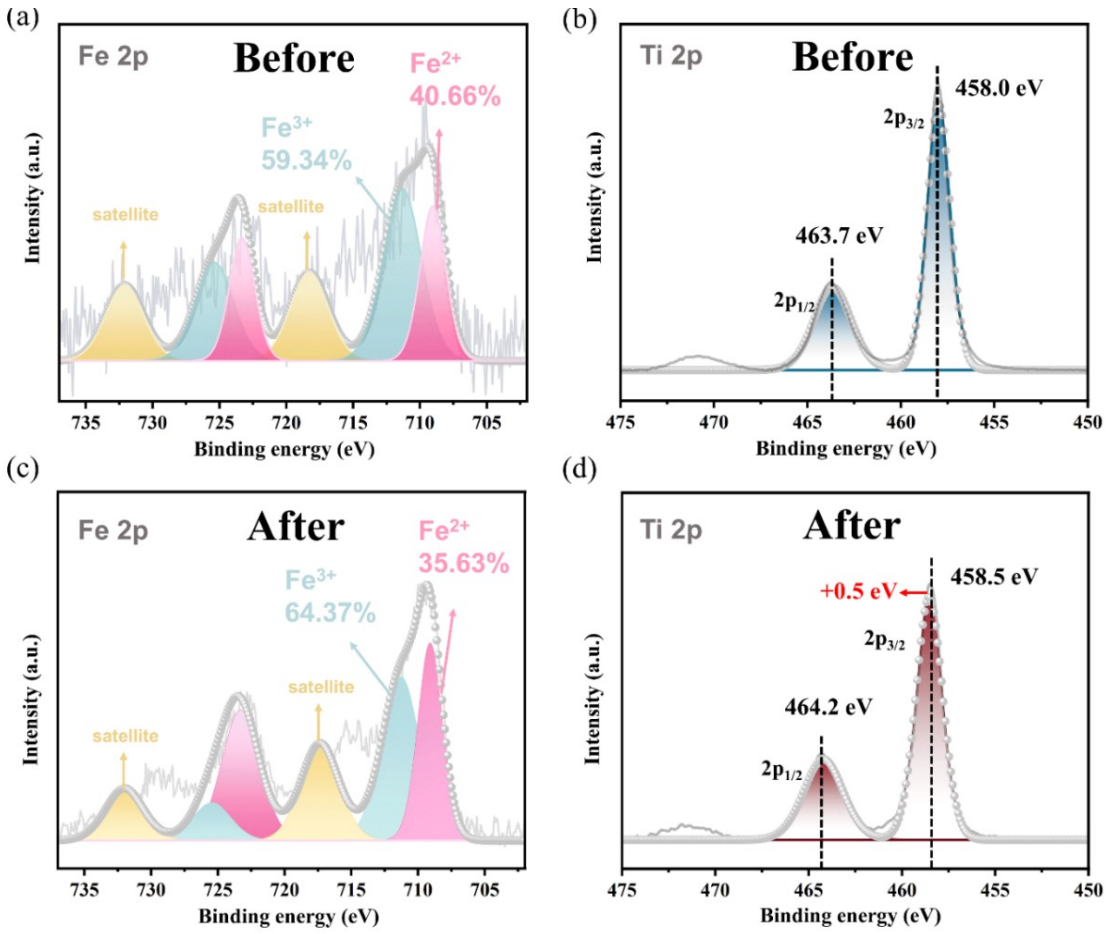

Fig. S14. XPS spectra of Fe 2p and Ti 2p for Fe/TiO_2 before (a and b) and after (c and d) the reaction.

Table S1. BET surface area of TiO_2, (x)Fe/TiO_2, and FeOOH.

Samples	Surface area (m^2/g)
TiO_2	417.9
0.2Fe/TiO_2	446.3
0.4Fe/TiO_2	385.3
0.6Fe/TiO_2	320.4

0.8Fe/TiO_2	**301.5**
FeOOH	**127.2**

Table S2. Air disinfection efficiency of ozone under different conditions.

Pathogens	O_3 Concentration (ppm)	Time (s)	Relative humidity (%)	Inactivation ratio (%)	Ref.
E. coli	15	1800	75-95	99.9	1
E. coli	20	1200	90	99.9	2
Influenza H3N2	20	3600	40-95	99.9	3
E. coli	50	10	50	95	4
MNV	100	1500	90	99.8	5
PEDV	100	1500	90	99.8	5
E. coli	300	15	18-20	95.8	6
E. coli	327	15	18-20	99.5	6
E. coli	389	15	18-20	97.9	6
E. coli	631	15	18-20	99.3	6
MS	100	1	-	90	7
MS	9000	1	-	99.9	7
E. coli	**8.2**	**5**	**93**	**99.97**	**This work**

Table S3. The O_{ads}/O_{latt} ratio of FeOOH and Fe/TiO_2.

Sample	O_{ads}/O_{latt} ratio

FeOOH	2.31
Fe/TiO_2	6.93

Table S4. The C_{dl} value and electrochemical surface area (ECSA) for FeOOH and Fe/TiO_2.

	FeOOH	Fe/TiO_2
C_{dl} ($\mu F\ cm^{-2}$)	35.5	65.3
ECSA (cm^2)	0.59	1.09

REFERENCES

1. J. Moat, J. Cargill, J. Shone and M. Upton, *Can. J. Microbiol.*, 2009, **55**, 928-933.

2. M. Sharma and J.B. Hudson, *Am. J. Infect. Control*, 2008, **36**, 559-563.

3. J. B. Hudson, M. Sharma and S. Vimalanathan, *Ozone: Sci. Eng.*, 2009, **31**, 216-223.

4. H.-L. Huang, M.-G. Lee and J.-H. Tai, *Aerosol Air Qual. Res.*, 2012, **12**, 73-82.

5. I. Falcó, W. Randazzo, G. Sánchez, J. Vilarroig, J. Climent, S. Chiva, A. Chica and J. Navarro-Laboulais, *J. Environ. Chem. Eng.*, 2021, **9**, 106217.

6. W.J. Kowalski, W.P. Bahnfleth and T.S. Whittam, *Ozone Sci. Eng.*, 1998, **20**, 205-221.

7. M.M. Kekez, S.A. Sattar, *Phys. Med. Biol.*, 1997, **42**, 2027.